ELSEVIER

A homology modeling method of an icosahedral viral capsid: Inclusion of surrounding protein structures

Teruyo Yoneda,* Shigetaka Yoneda,† Naoko Takayama,* Masako Kitazawa,* and Hideaki Umeyama*

**School of Pharmaceutical Sciences, Kitasato University, Tokyo, Japan*
†School of Science, Kitasato University, Kanagawa, Japan

A methodological development is presented for homology modeling of an icosahedrally symmetric assembly of proteins. In the method, a main-chain structure of an asymmetric unit of a protein assembly is constructed and structure refinement is performed, taking the surrounding symmetry-related proteins into consideration with rotational symmetry boundary conditions. To test the procedure, three models of a poliovirus capsid were constructed with different modeling conditions based on the X-ray structure of a rhinovirus capsid. Model S and model N were constructed with and without considering surrounding proteins, respectively. Model N2 was obtained by refinement in rotational symmetry boundary conditions of the structure of model N. The three models were compared with the X-ray structure of a poliovirus capsid. Root mean square deviations and C_α distances indicate that model S is the most accurate. Examination of the intermolecular short contacts indicates that model S and model N2 are superior to model N, because they do not make severe intermolecular short contacts. Symmetric intermolecular interactions are important for both the structural fragment search and energy minimization to predict better loop structures. The programs developed in this study are thus valuable in homology modeling of an icosahedral viral capsid. © *2000 by Elsevier Science Inc.*

Keywords: homology modeling, icosahedral capsid, poliovirus, protein assembly, rhinovirus

INTRODUCTION

One of the most important targets of modern pharmaceutical and biological studies is viruses. Especially, studies of viral capsids constitute a fundamental part of virus sciences. Many X-ray structures of capsids have been determined to design antiviral drugs and for theoretical and experimental studies of viral mechanisms.[1–6] Several dozens of structures related with capsids are now deposited in the Brookhaven Protein Data Bank.[7] However, a capsid is a typical large protein assembly, and X-ray analysis is still difficult and time consuming. Thus homology modeling methods[8–16] are important as a practical approach to predict capsid structures.

Homology modeling of capsids has a unique difficulty related to symmetric assembling. A capsid is composed of many identical copies of a unit called a "protomer," which is usually itself composed of a few protein molecules. Positions and orientations of protomers in a capsid are helically or icosahedrally symmetric. Thus a protomer of a capsid is surrounded by neighbor protomers under symmetric conditions and the symmetric neighbors influence the fidelity of the model, as described in the study of minimization and molecular dynamics simulation of the icosahedral capsid of human rhinovirus 14.[17] In their dynamics calculations, the deviation from the X-ray structure after 15 ps was 2.892 Å for the free-standing boundary and 1.694 Å for the full icosahedral boundary. They concluded that profound effects by the neighbor protomers may be seen in more detailed calculations. Thus the influence of neighbor protomers is expected to be important in homology modeling as well. However, to our knowledge, intermolecular interactions have not been calculated, nor have they been clearly described in homology modeling of a capsid,[10] and thus development of homology modeling to explicitly include intermolecular interactions is needed for virus capsid studies.

The advanced methodology used in the previous simulational studies of capsids can be used as a basis for developing homology modeling. In the earliest studies,[18–20] only a single protomer was simulated in vacuo because of the limited computer power available at that time. Later, calculations were carried out with water molecules, but were restricted to small regions near the binding sites of antiviral drugs.[21–28] Because the regions were often made of the fragments of several pro-

Color Plates for this article are on pages 137–142.

Corresponding author: Teruyo Yoneda, (present address) PharmaDesign, Inc., 4-2-10 Hatchobori, Chuo-ku, Tokyo 104-0032 Japan. Tel.: +81 3 3523 9630; fax: +81 3 3523 9631.

E-mail address: yoneda@pharmadesign.co.jp (T. Yoneda)

Journal of Molecular Graphics and Modelling 17, 114–119, 1999

655 Avenue of the Americas, New York, NY 10010

1093-3263/99/$–see front matter
PII S1093-3263(99)00024-8

tomers, the intermolecular interactions, if short range, were included correctly. More recently, calculations were performed on an assembly of several or all the protomers of a capsid.[25,29–32] In these studies, intermolecular interactions to a protomer were calculated from the atomic coordinates of the surrounding protomers in the assembly. This straightforward approach was also adopted in the refinement process of X-ray analysis.[33,34] In some of the studies using this approach, it was assumed that the assembly should be symmetric and that the surrounding protomer structures should be identical.

To use symmetry more effectively, the rotational symmetry boundary condition (RSBC) was proposed by Cagin, Holder, and Pettitt.[17] In RSBCs, an asymmetric unit of a capsid is adopted for a computational cell. Whereas simulation of liquid in periodic boundary conditions is performed within a periodic boundary box, simulation of a capsid in RSBC is performed within the computational cell of asymmetric unit. Intermolecular interactions are calculated with symmetric images of the computational cell. Because the number of atoms in this computational cell is equal to that of a protomer, simulations of a computational cell are equivalent to those of a single protomer. However, the shape of the computational cell is simpler and smoother than that of a protomer, and intermolecular interactions with symmetric images of the cell can be calculated much faster. Thus RSBCs are effective for calculating intermolecular interactions. The first study of energy minimization and molecular dynamics simulation in RSBCs was performed by Cagin et al.,[17] and a strict formulation of RSBC and a longer simulation were presented later.[35,36]

The most straightforward approach to construct a capsid structure is to repeat the conventional homology modeling procedure of an isolated protein. First, a tertiary structure of a protomer is constructed by the conventional homology modeling procedure. Using the protomer structure, an assembly of several protomers is generated. The structure of the assembly is refined by energy minimization or molecular dynamics simulations without symmetry constraints. When a loop structure is not appropriately selected, short contacts between the loop and a neighbor protomer still remain after the refinement. To relax the short contacts, the loop structure is changed with another loop structure, the assembly is reconstructed, and the refinement is conducted. This procedure is repeated until the short contacts are removed. When a loop makes short contacts with its symmetric images of neighbor protomers, the iterative procedure described above is also conducted. Furthermore, to remove this type of short contacts, many iteration cycles may be necessary.

In this study, we present the development of a suite of programs to model an icosahedral viral capsid. With these programs, a main-chain structure of a protomer of an icosahedral capsid is constructed by considering the surrounding symmetry-related protomers, which are generated in RSBCs. The model structure is refined by energy minimization in RSBCs. With this modeling procedure the iteration described above is not necessary, because a structural change in the center protomer is reflected simultaneously in symmetry-related protomers. To test the new procedure, we constructed a tertiary structure of a capsid of poliovirus 1 based on the X-ray structure of that of rhinovirus 14.

Rhinovirus 14 and poliovirus 1, both of which belong to the *Picornaviridae*, are icosahedral nonenveloped viruses. A capsid of rhinovirus or poliovirus is composed of 60 copies of one protomer, which in turn is composed of the four coat proteins: VP1, VP2, VP3, and VP4. The numbers of amino acid residues of the four proteins of rhinovirus 14 are similar to those of poliovirus 1, and the sequence identities of these proteins are relatively high between the two viruses: VP1, 44%; VP2, 56%; VP3, 43%; and VP4, 57%. The X-ray structure of rhinovirus 14 was determined by Rossmann et al.,[3] and that of poliovirus 1 by Hogle et al.[4] Both viruses are about 300 Å in diameter. These two viruses are suitable for the first test of the new approach, as the sizes of the capsids are almost the same, the amino acid sequences are homologous, and the X-ray structures are known.

The homology model of poliovirus 1 constructed considering surrounding proteins will be called "model S" in this article. For comparison, model building without considering surrounding proteins was conducted to give what we call "model N." The modeling procedure for the third model, "model N2," is the same as that of model N, except that the initial structure was refined by energy minimization in RSBCs. The three models were compared with the X-ray structure of poliovirus 1 to assess the accuracy of the method of this study.

MATERIALS AND METHODS

Rotation matrices of capsids of rhinovirus and poliovirus

The X-ray coordinates of rhinovirus 14, 4RHV,[3] were used for the reference structure in the homology modeling. The model structure of a poliovirus capsid was compared with the X-ray coordinates of poliovirus 1, 2PLV.[4] Both sets of coordinates are available from the Brookhaven Protein Data Bank.[7] The rotation matrices required to create an entire capsid from the coordinates of one protomer are included in the respective PDB files.

Since the coordinate axes adopted in 4RHV are different from those in 2PLV, the following rotation matrix [Eq. (1)] was applied to 4RHV to be superimposed on 2PLV. By the rotation with the inverse matrix of this, 2PLV is superimposed on 4RHV.

$$\begin{bmatrix} -(5^{0.5}+1)/4 & -(5^{0.5}-1)/4 & 0.5 \\ 0.5 & -(5^{0.5}+1)/4 & (5^{0.5}-1)/4 \\ (5^{0.5}-1)/4 & 0.5 & (5^{0.5}+1)/4 \end{bmatrix}$$

Modeling procedure with symmetry-related protomers

The present procedure is a further development of our in-house modeling procedure.[13–16]

Amino acid sequences of the four coat proteins of the target protein, poliovirus, were aligned to those of the reference protein, rhinovirus, by the method of hydrophobic core scores.[37] In this method, the parameters of the hydrophobic core scores were calculated by cluster analysis of hydrophobic residues of the reference structure and were considered in the alignment process by a variant of the Needleman and Wunsch algorithm.[38] By this method, insertions and deletions in the alignment were placed out of the hydrophobic core of the reference structure.[37] We considered surrounding protomers in the calculation of the hydrophobic core scores using the RSBCs. The RSBC is a method by which to use an asymmetric

unit for a computational cell, as described above (see Introduction).

The main-chain structures of the four coat proteins of the reference structure were used for those of the target proteins, except for insertion/deletion regions. For insertion/deletion regions, structural fragments were searched in our structural fragment database made from all the PDB entries. Short contacts of these fragments were checked with surrounding proteins. Here also the symmetry-related protomers were generated in RSBCs. As all equivalent insertion/deletion regions were simultaneously replaced with the fragment being examined, short contacts between a fragment and its symmetric images were removed. For example, a fivefold axis is surrounded by five VP1s in rhinovirus and poliovirus. Since a loop around a fivefold axis might make short contacts with its symmetric images, the five identical insertion/deletion regions were replaced by the fragment. Sequence identity and structural fitness of the fragments were also examined. Then, the most appropriate fragment was chosen as a main-chain structure for an insertion/deletion region.

The side-chain structures of the conserved residues of the reference were used as those of the target without modification. For the other amino acids of the target, side-chain conformations were determined by random search of torsional angles by program KMNT. (KMNT does not consider the surrounding proteins.) The structure obtained was energy minimized by the conjugate gradient method in RSBCs. APRICOT[39] was used for this minimization. APRICOT is a program that we have developed and is one of the MD simulation programs such as AMBER,[40] CHARMM,[41] GROMOS,[42] etc. APRICOT has been used for calculations of many biomolecules[16,43–46] and the RSBC method has already been implemented.[35,36] The AMBER united-atom force field[47] was used. The residue-based cutoff of 8 Å and the dielectric constant ϵ of 4.0 were adopted. Backbone atoms were kept to their initial positions by constraints at the first stage of minimization, then the constraints were weakened stepwise, and finally all positional constraints were removed. The convergence criterion of the minimization was the root mean square of atomic forces smaller than 0.2 kcal/mol/Å. We call this model "model S."

To clarify influence from the surrounding protomers, another model of a poliovirus capsid named "model N" was built. Each of the four coat proteins of model N was constructed and energy minimized according to the same procedure as that for model S, except that the surrounding proteins were not considered. Energy minimization was carried out by APRICOT without RSBCs.

Furthermore, the initial structures of the four proteins of model N were overlaid to 4RHV by least square fitting of each coat protein, and then the obtained protomer structure was energy minimized in RSBCs. This third model was named "model N2." The modeling procedure for model N2 is the same as that of model N, except that the initial structure was refined by energy minimization in RSBCs.

RESULTS AND DISCUSSION

Three kinds of alignments of poliovirus 1 to rhinovirus 14 are shown in Color Plate 1. The alignment of the first line (4RHV) to the fourth line (2PLV) is a structural alignment of rhinovirus to poliovirus and was determined by comparing the two X-ray structures of 4RHV and 2PLV. The structural alignment was made when the modeling was finished. As seen in the structural alignment of VP1, the 11 residues of poliovirus, denoted by an arrow, should be inserted where the coordinates of rhinovirus are not determined experimentally. However, in the alignments used for models S, N, and N2, an insertion was placed where the coordinates of rhinovirus are determined as indicated by asterisks. This misalignment was mainly caused by the identical sequence of TV, written in green in the alignment. The structural fragment search was performed for the insertion/deletion regions denoted by underlines in Color Plate 1. Short contacts between the fragment and the surrounding proteins were checked computer graphically for model S, as shown in Color Plate 2.

The three models were compared with the original X-ray structure, 2PLV. The comparison with the original X-ray structure is better than comparison with an energy-minimized X-ray structure, because results of energy minimization depend very much on calculational conditions and the ultimate purpose of modeling is to predict X-ray structures. Furthermore, difference from the X-ray structure is widely used as a good criterion by which to estimate the accuracy of structure prediction.[8] Root mean square deviations (RMSDs) after least square fitting of each coat protein are shown in Table 1. The RMSDs of model S are small and comparable to the RMSDs of isolated protein models.[13,15] Among the three models, model S is the most accurate, and the RMSDs for VP1 and VP2 of model S in particular are smaller than those of models N and N2. Model N2 is second best, and model N is the worst.

The C_α distances between each model and 2PLV were calculated after least square fitting of the main-chain atoms of the template regions as shown in Color Plate 3. "Template regions" are all regions except insertion/deletion regions. The structural differences in the template regions among the three models were caused by energy minimization, because identical main-chain structures of 4RHV were commonly used for the template regions in the three models. The C_α distances between the X-ray structures, 2PLV and 4RHV, are also plotted in Color Plate 3. In the insertion region before residue number 200 of VP2, the reference structure, 4RHV, is closer to 2PLV than any of the three models. This was caused by misalignment of an insertion. While eight residues were inserted at one position in the structural alignment between 2PLV and 4RHV, they were inserted separately at four positions for model S and at three positions for model N and model N2, as shown in Color Plate 1b. No data are plotted from residues 161 to 168 for 4RHV in Color Plate 3b, because the corresponding residues do not exist in 4RHV. The order of accuracy among the three models is the

Table 1. RMSDs (Å) between model and x-ray structure[a]

Model	VP1	VP2	VP3	VP4
S	2.4 (2.9)[b]	2.8 (3.3)	1.3 (2.2)	1.6 (2.9)
N2	3.0 (3.5)[b]	3.3 (3.8)	1.3 (2.2)	1.5 (2.8)
N	3.4 (3.9)[b]	3.4 (4.0)	1.9 (2.6)	1.7 (3.0)

[a] Numbers represent the RMSDs of main-chain atoms, and those in parentheses represent the RMSDs of all nonhydrogen atoms.
[b] The first 24 residues of the N terminus were excluded from RMSD calculation. The RMSDs of a whole chain of VP1 were 5.7 (6.0) for model S, 5.9 (6.1) for model N2, and 6.0 (6.2) for model N.

same as that derived from the RMSDs. Although model S is better than the other two models for most insertion/deletion regions, these regions are still not predicted well. Prediction of loop structures is difficult even in homology modeling of an isolated protein.[9]

The backbone structures of the three models and 2PLV are shown in Color Plate 4. Least square fitting was done for the main-chain atoms of the template regions. For model N the four coat proteins were overlaid to the X-ray structure by least square fitting of each coat protein. The large deviations of VP1 of the three models, denoted by an asterisk, are due to the misalignment of the N terminus of VP1 as discussed above.

Intramolecular short contacts between nonhydrogen atoms, whose interatomic distances are shorter than 2.0 Å, were not observed in any coat proteins of the three models and 2PLV. Intermolecular distances between nonhydrogen atoms were calculated, including surrounding protomers, and the numbers of the intermolecular short contacts are plotted along with contact distances for each coat protein as shown in Color Plate 5. Color Plate 5 shows that model N is the worst among the three models, because it makes severe intermolecular short contacts; there are three severe intermolecular short contact sites whose main-chain interatomic distances are shorter than 2.0 Å. As for model S and model N2, such severe intermolecular short contacts do not exist. The three short contact sites of model N are denoted as site I, site II, and site III as shown in Figure 1. Site I is an insertion region of VP1 as indicated in Color Plate 1 and makes short contacts with the residues from 144 to 147 of VP2. Color Plate 3 shows that site I deviates largely from the structure of 2PLV. Because the structural fragments of model N were searched without surrounding proteins, a loop making short contacts was selected for model N. Site II is an insertion region of VP3 and makes short contacts with a deletion region of the C terminal of VP1 as shown in Color Plate 1. Because site II of VP3 deviated more than that of the deletion region of VP1 as shown in Color Plate 3, the structural fragment selected as site II was not appropriate. Although the initial structures of model N and model N2 before minimization were the same, the short contacts of sites I and II were removed in model N2 during energy minimization in RSBCs. Site III is near a fivefold axis and makes short contacts with its symmetric images. This site is not an insertion/deletion region but a template region as shown in Color Plate 3. Since site III is at the N-terminal extension of VP3, as shown in Color Plate 4, it was moved largely from the initial position during minimization without surrounding proteins. The short contacts of site III were not caused in model N2 owing to the minimization in RSBCs.

Loop structures play important roles in the life of poliovirus and rhinovirus: antigenic sites reside on the outer surface of a capsid, and an elaborate network that stabilizes the virion decorates the inner surface.[5] Both the antigenic sites and the network are composed mainly of loops of neighbor coat proteins. Loops also compose a part of the "canyon," which is thought to bind cellular receptors, and the "drug-binding pocket," which binds a hydrophobic ligand (or "pocket factor").

The antigenic sites 1, 2, 3A, and 3B determined for poliovirus[48] are shown in blue in the sequence of 2PLV in Color Plate 1. Almost of these antigenic sites are in or near insertion/deletion regions, and two of these regions include the short contact sites of model N discussed above. An insertion region of the G–H loop of VP1, which comprises antigenic site 2, includes the short contact site I, and another insertion region of the N-terminal extension of VP3, in which the antigenic site 3A is located, includes the short contact site II.

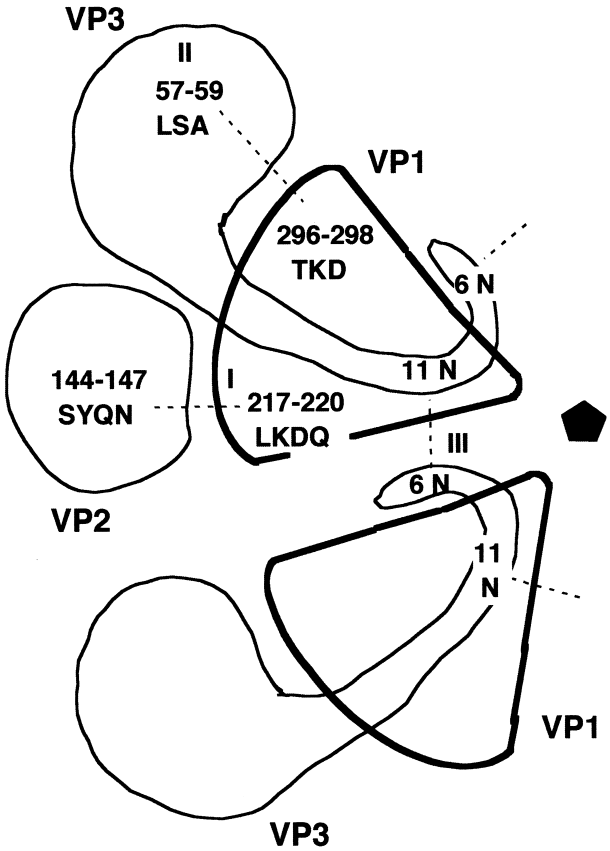

Figure 1. Schematic drawing of intermolecular short contacts in model N. Residue pairs closer than 2.0 Å between main-chain atoms are shown. A contacting residue is denoted with a residue number and a one-letter code of an amino acid. Three short contact sites are denoted with roman figures. VP1 and VP3 of a neighbor protomer are drawn to indicate the site III around a fivefold axis, which is denoted by a filled pentagon. VP4 is not shown because no short intermolecular contacts are observed.

In terms of RMSDs, C_α distances, and intermolecular short contacts, model S is the most accurate among the three models. Thus inclusion of surrounding protein structures improved the accuracy of homology modeling of the viral capsid. Even when a model was constructed without surrounding proteins, structure refinement by energy minimization in RSBCs improved the model. However, a structural fragment search with surrounding proteins in RSBCs gave more appropriate loop structures. So both a structural fragment search and energy minimization must be conducted, taking symmetry into consideration.

Our modeling procedure is a combination of the traditional modeling procedure and the method of RSBC. If other modeling methods[49,50] were combined with the RSBC, good structure predictions would similarly be expected. Thus consideration of surrounding protein structures is important for any modeling procedures of protein assemblies.

When modeling a protein assembly, it is important that any structural change in an asymmetric unit be reflected simultaneously in the symmetry-related proteins in order to remove short contacts between a fragment and its symmetric images. The present procedure of structure fragment search and energy minimization enables simultaneous changes of identical structures. However, the present modeling procedure also has its weaknesses. Although model S does not have severe intermolecular short contacts, C_α distances for insertion/deletion regions are not small, as shown in Color Plate 3. This is caused partly by inappropriate alignment of amino acid sequences. The two serious misalignments of this modeling were discussed above. Another problem is related to construction of the loop structures. This is a difficult problem even in the homology modeling of isolated proteins. These problems were not solved in this study.

CONCLUSIONS

Comparisons of the three models of a poliovirus capsid with the X-ray structure indicate that model S, which is constructed by taking symmetry into consideration, is the most accurate model. This means that both a structural fragment search and energy minimization must be conducted, taking symmetry into consideration. Thus the procedure of this study is valuable in homology modeling of an icosahedral viral capsid.

ACKNOWLEDGMENTS

We thank Dr. H. Komooka, Kitasato University, for use of the program HOFILE to calculate hydrophobic cores, and Dr. H. Kaneko, NEC Corporation, for the use of program KMNT. This work was supported by a Grand-in-Aid from the Ministry of Education, Science, Sports and Culture, Japan.

REFERENCES

1 Bloomer, A.C., Champness, J.N., Bricogne, G., Staden, R., and Klug, A. Protein disk of tobacco mosaic virus at 2.8 Å resolution showing the interactions within and between subunits. *Nature (London)* 1978, **276,** 362–368
2 Harrison, S.C., Olson, A., Schutt, C.E., Winkler, F.K., and Bricogne, G. Tomato bushy stunt virus at 2.9 Å resolution. *Nature (London)* 1978, **276,** 368–373
3 Rossmann, M.G., Arnold, E., Erickson, J.W., Frankenberger, E.A., Griffith, J.P., Hecht, H.-J., Johnson, J.E., Kamer, G., Luo, M., Mosser, A.G., Rueckert, R.R., Sherry, B., and Vriend, G. Structure of a human common cold virus and functional relationship to other picornaviruses. *Nature (London)* 1985, **317,** 145–153
4 Hogle, J.M., Chow, M., and Filman, D.J. Three-dimensional structure of poliovirus at 2.9 Å resolution. *Science* 1985, **229,** 1358–1365
5 Wien, M.W., Chow, M., and Hogle, J.M. Poliovirus: New insights from an old paradigm. *Structure* 1996, **4,** 763–767
6 Diana, G.D., McKinlay, M.A., and Treasurywala, A. The use of structural information in the design of picornavirus capsid binding agents. In: *Structural Biology of Viruses* (Chiu, W., Burnett, R.M., and Garcea, R.L., eds.). Oxford University Press, New York, 1997, pp. 432–450
7 Bernstein, F.C., Koetzle, T.F., Williams, G.J.B., Meyer, E.F., Jr., Brice, M.D., Rodgers, J.R., Kennard, O., Shimanouchi, T., and Tasumi, M. The Protein Data Bank: A computer-based archival file for macromolecular structures. *J. Mol. Biol.* 1977, **112,** 535–542
8 Johnson, M.S., Srinivasan, N., Sowdhamini, R., and Blundell, T.L. Knowledge-based protein modeling. *Crit. Rev. Biochem. Mol. Biol.* 1994, **29,** 1–68
9 Venclovas, C., Zemla, A., Fidelis, K., and Moult, J. Criteria for evaluating protein structures derived from comparative modeling. *Proteins* 1997, **S1,** 7–13
10 Liljas, L., Lindberg, A.M., and Pettersson, U. Modelling of the tertiary structure of coxsackievirus B3 from the structure of poliovirus and rhinovirus. *Scand. J. Infect. Dis.* 1993, **S88,** 15–24
11 Akahane, K., Umeyama, H., Nakagawa, S., Moriguchi, I., Hirose, S., Iizuka, K., and Murakami, K. Three-dimensional structure of human renin. *Hypertension* 1985, **7,** 3–12
12 Shiratori, Y., Nakagawa, S., Hori, H., Murakami, K., and Umeyama, H. Protein modeling of human prorenin using the molecular dynamics method. *J. Mol. Graphics* 1990, **8,** 163–167
13 Kajihara, A., Komooka, H., Kamiya, K., and Umeyama, H. Protein modelling using a chimera reference protein derived from exons. *Protein Eng.* 1993, **6,** 615–620
14 Matsui, I., Yoneda, S., Ishikawa, K., Miyairi, S., Fukui, S., Umeyama, H., and Honda, K. Roles of the aromatic residues conserved in the active center of *Saccharomycopsis* α-amylase for transglycosylation and hydrolysis activity. *Biochemistry* 1994, **3,** 451–458
15 Yoneda, T., Komooka, H., and Umeyama, H. A computer modeling study of the interaction between tissue factor pathway inhibitor and blood coagulation factor Xa. *J. Protein Chem.* 1997, **16,** 597–605
16 Takeda-Shitaka, M., and Umeyama, H. Elucidation of the cause of for reduced activity of abnormal human plasmin containing an Ala^{55}-Thr mutation: Importance of highly conserved Ala^{55} in serine proteases. *FEBS Lett.* 1998, **425,** 448–452
17 Cagin, T., Holder, M., and Pettitt, B.M. A method for modeling icosahedral virions: Rotational symmetry boundary conditions. *J. Comput. Chem.* 1991, **12,** 627–634
18 Lau, W.F., Pettitt, B.M., and Lybrand, T.P. Molecular dynamics of coat proteins of the human rhinovirus. *Mol. Simulation* 1988, **1,** 385–398
19 Lau, W.F., and Pettitt, B.M. Dynamics of an oxazole compound bound to a common cold virus. *J. Am. Chem. Soc.* 1989, **111,** 4111–4113
20 Lau, W.F., and Pettitt, B.M. Selective elimination of interactions: A method for assessing thermodynamic contributions to ligand binding with application to rhinovirus antivirals. *J. Med. Chem.* 1989, **32,** 2542–2547
21 Lybrand, T.P., Lau, W.F., McCammon, J.A., and Pettitt, B.M. Molecular dynamics studies on antiviral agents: Thermodynamics of solvation and binding. In: *Protein Structure, Folding, and Design* (Oxender, D.L., ed.), Vol. 2. Alan R. Liss, New York, 1987, pp. 227–233
22 Lybrand, T.P., and McCammon, J.A. Computer simulation study of the binding of an antiviral agent to a sensitive and a resistant human rhinovirus. *J. Comput.-Aided Mol. Design* 1988, **2,** 259–266
23 Wade, R.C., and McCammon, J.A. Binding of an antiviral agent to a sensitive and a resistant human rhinovirus. Computer simulation studies with sampling of

amino acid side-chain conformations. I. Mapping the rotamers of residue 188 of viral protein 1. *J. Mol. Biol.* 1992, **225,** 679–696
24 Wade, R.C., and McCammon, J.A. Binding of an antiviral agent to a sensitive and a resistant human rhinovirus. Computer simulation studies with sampling of amino acid side-chain conformations. II. Calculation of free-energy differences by thermodynamic integration. *J. Mol. Biol.* 1992, **255,** 697–712
25 Guha-Biswas, M., Holder, M., and Pettitt, B.M. On the mechanism of HRV-14 antiviral compounds: "Slow growth" as a conformational search procedure. *J. Med. Chem.* 1993, **36,** 3489–3495
26 Phelps, D.K., and Post, C.B. A novel basis for capsid stabilization by antiviral compounds. *J. Mol. Biol.* 1995, **254,** 544–551
27 Joseph-McCarthy, D., Hogle, J.M., and Karplus, M. Use of the multiple copy simultaneous search (MCSS) method to design a new class of picornavirus capsid binding drugs. *Proteins* 1997, **29,** 32–58
28 Phelps, D.K., Rossky, P.J., and Post, C.B. Influence of an antiviral compound on the temperature dependence of viral protein flexibility and packing: A molecular dynamics study. *J. Mol. Biol.* 1998, **276,** 331–337
29 Mathiowetz, A.M., Jain, A., Karasawa, N., and Goddard, W.A., III. Protein simulations using techniques suitable for very large systems: The cell multipole method for nonbond interactions and the Newton–Euler inverse mass operator method for internal coordinate dynamics. *Proteins* 1994, **20,** 227–247
30 Vaidehi, N., and Goddard, W.A., III. The pentamer channel stiffening model for drug action on human rhinovirus HRV-1A. *Proc. Natl. Acad. Sci. U.S.A.* 1997, **94,** 2466–2471
31 van Vlijmen, H.W.T., Curry, S., Schaefer, M., and Karplus, M. Titration calculation of foot-and-mouth disease virus capsids and their stabilities as a function of pH. *J. Mol. Biol.* 1998, **275,** 295–308
32 Reddy, V.S., Giesing, H.A., Morton, R.T., Kumar, A., Post, C.B., Brooks, C.L., III, and Johnson, J.E. Energetics of quasiequivalence: Computational analysis of protein–protein interactions in icosahedral viruses. *Biophys. J.* 1998, **74,** 546–558
33 Bruenger, A.T., Karplus, M., and Petsko, G.A. Crystallographic refinement by simulated annealing: Application to crambin. *Acta Crystallogr.* 1989, **A45,** 50–61
34 Weis, W.I., Bruenger, A.T., Skehel, J.J., and Wiley, D.C. Refinement of the influenza virus hemagglutinin by simulated annealing. *J. Mol. Biol.* 1990, **212,**737–761
35 Yoneda, S., Kitazawa, M., and Umeyama, H. Molecular dynamics simulation of a rhinovirus capsid under rotational symmetry boundary conditions. *J. Comput. Chem.* 1996, **17,** 191–203
36 Yoneda, S. A further implementation of the rotational symmetry boundary conditions for calculations of $P4_32_12$ symmetry crystals. *J. Mol. Graphics Modelling* 1997, **15,** 233–237
37 Kanaoka, M., Kishimoto, F., Ueki, Y., and Umeyama, H. Alignment of protein sequences using the hydrophobic core scores. *Protein Eng.* 1989, **2,** 347–351
38 Needleman, S.B., and Wunsch, C.D. A general method applicable to the search for similarities in the amino acid sequence of two proteins. *J. Mol. Biol.* 1970, **48,** 443–453
39 Yoneda, S., and Umeyama, H. Free energy perturbation calculations on multiple mutation bases. *J. Chem. Phys.* 1992, **97,** 6730–6736
40 Pearlman, D.A., Case, D.A., Caldwell, J.W., Ross, W.S., Cheatham, T.E., III, Ferguson, D.M., Seibel, G.L., Singh, U.C., Weiner, P.K., and Kollman, P.A. *AMBER 4.1*. University of California, San Francisco, 1995.
41 Brooks, B.R., Bruccoleri, R.E., Olafson, B.D., States, D.J., Swaminathan, S., Karplus, M. CHARMM: A program for macromolecular energy, minimization and dynamics calcultions. *J. Comput. Chem.* 1983, **4,** 187–217
42 van Gunsteren, W.F., Billeter, S.R., Eising, A.A., Huenenberger, P.H., Krueger, P., Mark, A.E., Scott, W.R.P., and Tironi, I.G. *Biomolecular simulation: The GROMOS96 manual and user guide*. BIOMOS, Zurich, Switzerland, 1996
43 Kajihara, A., Komooka, H., Kamiya, K., Yoneda, T., Yoneda, S., Nakamura, M., Shimizu, T., and Umeyama, H. Three-dimensional model of human PAF receptor. *J. Lipid Mediators Cell Signalling*, 1994, **9,** 185–196
44 Higo, J., and Umeyama, H. Protein dynamics determined by backbone conformation and atom packing. *Protein Eng.*, 1997, **10,** 373–380
45 Takeda-Shitaka, M., and Umeyama, H. Effect of exceptional valine replacement for highly conserved alanine55 on the catalytic site structure of chymotrypsin-like serine protease. *Chem. Pharm. Bull.* 1998, **46,** 1343–1348
46 Takeda-Shitaka, M., Kamiya, K., Miyata, T., Ohkura, N., Madoiwa, S., Sakata, Y., and Umeyama, H. Structural studies of the interactions of normal and abnormal human plasmins with bovine basic pancreatic trypsin inhibitor. *Chem. Pharm. Bull.* 1999, **47,** 322–328
47 Weiner, S.J., Kollman, P.A., Case, D.A., Singh, U.C., Ghio, C., Alagona, G., Profeta, S, Jr., and Weiner, P. A new force field for molecular mechanical simulation of nucleic acids and proteins. *J. Am. Chem. Soc.* 1984, **106,** 765–784
48 Page, G.S., Mosser, A.G., Hogle, J.M., Filman, D.J., Rueckert, R.R., and Chow, M. Three-dimensional structure of poliovirus serotype 1 neutralizing determinants. *J. Virol.* 1988, **62,** 1781–1794
49 Sali, A., and Blundell, T.L. Comparative protein modelling by satisfaction of spatial restraints. *J. Mol. Biol.* 1993, **234,** 779–815
50 Ogata, K., and Umeyama, H. The role played by environmental residues on sidechain torsional angles within homologous families of proteins: A new method of sidechain modeling. *Proteins* 1998, **31,** 355–369